Chemical Engineering Journal 498 (2024) 154988

Contents lists available at ScienceDirect

Chemical Engineering Journal

journal homepage: www.elsevier.com/locate/cej

Beyond Plastic: Oleogel as gel-state biodegradable thermoplastics

Leonardo Lamanna [a,*], Gabriele Corigliano [b,c], Athira Narayanan [a], Stefania Villani [a], Marco Friuli [a], Francesco P. Chietera [a], Benedetta Di Chiara Stanca [d], Laura Giannotti [e], Luisa Siculella [e], Riccardo Colella [a], Luca Catarinucci [a], Athanassia Athanassiou [b], Pietro Cataldi [b], Christian Demitri [e], Mario Caironi [f], Alessandro Sannino [e]

[a] Department of Engineering for Innovation, Campus Ecotekne, University of Salento, Via Per Monteroni, 73100 Lecce, Italy
[b] Smart Materials, Istituto Italiano di Tecnologia, Via Morego 30, 16163 Genoa, Italy
[c] Department of Earth and Environmental Sciences (DISAT), University of Milan – Bicocca, Piazza Della Scienza 20126 Milan, Italy
[d] Department of Biological and Environmental Sciences and Technologies, University of Salento, Via Per Monteroni 73100 Lecce, Italy
[e] Department of Experimental Medicine, University of Salento, Via Per Monteroni 73100 Lecce, Italy
[f] Center for Nano Science and Technology, Istituto Italiano di Tecnologia, Via Rubattino 81, 20134 Milan, Italy

ARTICLE INFO

Keywords:
Bioplastic
Oleogel
Green packaging
Green electronics
Biocompatible materials
Gel-state thermoplastic

ABSTRACT

The crisis of plastic waste highlights the urgent need for sustainable alternatives. Bioplastics are seen as a potential solution; however, challenges persist as many are still derived from petroleum, lack biodegradability, or fall short in essential properties such as mechanical strength, chemical stability, and ease of processing. This study pioneers the use of ethyl cellulose-based oleogels as bioderived and biodegradable thermoplastics. These groundbreaking bioplastics, obtained from renewable sources and waste oils, represent an environmentally friendly and high-performance alternative to traditional plastics. The bioplastic named OleoPlast is processed at temperatures ranging from 130 to 165 °C, utilizing different biobased oils and adjusting the oil-to-polymer ratio from 10:3.5 to 1:2. This process yields a high level of versatility, offering broad opportunities for customized applications in both research and industry. Remarkable stability under harsh environmental conditions and biocompatibility pave the way for the adoption of such bioplastics in biocomposite structures, food packaging, green electronics, and tissue engineering. Scalability is ensured by compatibility with both large-scale and high-resolution manufacturing processes, including injection and compression molding, computer numeric control (CNC) milling, and 3D fusion deposition modeling.

Overall, this work lays the foundation for a new class of gel-state bioplastics, favoring the transition from traditional thermoplastics to sustainable options with vast perspectives of further exploration and customization in both laboratory and industrial environments.

1. Introduction

Traditional petroleum-based plastics, known for their affordability and durability, are extensively utilized in various industries, including packaging, construction, electronics, and aerospace [1–4]. Such plastics pose a significant environmental threat due to their slow degradation, spanning hundreds to thousands of years. Predictions suggest an alarming accumulation of approximately 11 billion tons of plastic waste in both landfills and the oceans by 2025 [5], driving another critical issue of our century: the proliferation of microplastics and their bioaccumulation in different organisms, including humans [6]. Starting from '70 s/'80 s, recycling programs were implemented to address the issue. However, the scale of the problem makes it evident that recycling is an insufficient mitigation measure [7]. Different plastics require separate recycling streams, which frequently results in higher costs than using virgin plastic. Additionally, the recycling process often degrades the quality of the plastic, requiring the addition of additives to restore its original properties [8].

Bioplastics have been proposed as a potential solution to address the challenges posed by traditional plastics [9,10]. Bioplastics, derived from renewable resources or produced through biological processes, provide substantial benefits, including a reduced footprint on both production workflows and waste management systems, aligning with the Sustainable Development Goals outlined by the United Nations [11]. Currently,

* Corresponding author.
E-mail address: leonardo.lamanna@unisalento.it (L. Lamanna).

https://doi.org/10.1016/j.cej.2024.154988
Received 20 May 2024; Received in revised form 1 August 2024; Accepted 18 August 2024
Available online 19 August 2024
1385-8947/© 2024 The Authors. Published by Elsevier B.V. This is an open access article under the CC BY license (http://creativecommons.org/licenses/by/4.0/).

bio-based bioplastics represent approximately 2 % of the global plastics production [12]. Nevertheless, not all bioplastics are inherently biodegradable and most of them still face limitations in terms of stability, mechanical properties, processability, and recycling [10,13]. Moreover, it is crucial to develop simple, solvent-free and sustainable methods for fabricating bioplastics using abundant natural resources [14]. While mechanical strength and robustness during use are a prerequisite and an ongoing challenge for bio-based bioplastics, a delicate trade-off with biodegradability and recyclability at the end of their lifespan must be found to ensure sustainability.

A critical consideration in the implementation and development of new bioplastics is their compatibility with existing large-scale manufacturing techniques for plastics and composites, such as injection and compression molding, as well as extrusion. This entails the need for a thermoplastic material with distinct melting and degradation temperatures, coupled with favorable rheological properties. Concurrently, the use of thermoplastic materials should ensure the adaptability of bioplastics to high-resolution prototyping techniques, including micro-compression molding and 3D printing. Such a level of versatility would facilitate seamless adoption across a broad spectrum of production and prototyping workflows, ensuring easy integration into existing production lines.

As the most widespread natural polymer, cellulose is earmarked as the leading material for future biodegradable bioplastics innovations [3,15]. However, its high degree of crystallinity poses challenges as it is insoluble in common solvents and prone to strong degradation during the melting process [16,17]. Despite cellulose derivatives have been studied for over a century, they face limitations in thermal processability and often exhibit poor mechanical properties due to their susceptibility to moisture and UV light [15,18]. Ethyl cellulose (EC) stands out as an exception to many of these limitations [19,20]. Being hydrophobic, it can be solubilized in oils above its glass transition temperature, resulting in the formation of stable oleogels, i.e. three-dimensional polymer networks that immobilize oils [21,22], similarly to how hydrogel traps water molecules [23].

Currently, oleogels are mainly used in the food industry as functional ingredients to enhance the texture, stability, and sensory properties of food products [24–27]. They have been employed to improve the mouth feel creaminess, and stability of various food formulations, including spreads, bakery products, confectionery, and dressings. A key advantage of oleogels, setting them apart from hydrogels, lies in their remarkable thermal and chemical stability, effectively preventing issues tied to evaporation. Additionally, oleogels offer a versatile platform for incorporating a wide array of hydrophobic molecules. These unique features allow precise modifications of the mechanical, physical, and chemical properties.

Here we introduce ethyl cellulose-based oleogels as the first eco-friendly, gel-state thermoplastics. The exploitation of oleogels as bioplastics represents a unique and captivating avenue, offering an unconventional and promising alternative that has yet to be investigated, with far-reaching implications for material science and engineering, as well as for diverse industries seeking sustainable and scalable solutions.

This study investigates the development and evaluation of EC-based oleogels, hereafter referred as OleoPlast, which is fully biobased and produced using a range of vegetable oils (sunflower, soybean, and peanut) with different EC ratios. The research aims to understand how these factors influence key properties such as melting temperature, processability, and mechanical performance. Techniques including injection molding, compression molding, CNC milling, extrusion, and 3D printing are utilized to explore the manufacturing flexibility and potential applications of OleoPlast. The study also highlights the environmental benefits of the material, including its recyclability, use of exhausted oil, and biodegradability, show up its alignment with circular economy principles. Proofs of concept have also been developed to demonstrate the versatility of OleoPlast in various applications, such as biofiber-reinforced composites, food packaging, green electronics, and innovative building materials for tissue engineering scaffolds.

2. Results and discussion

OleoPlast was produced through a straightforward method involving the hot mixing of EC with vegetable oil at 165 °C until a clear and viscous solution was obtained. Detailed production protocol is reported in material and method section. Widespread and cost-effective vegetable oils – sunflower (SF), soybean (SB), and peanut (PEA) – were used in this study to develop an entirely biobased material. Additionally, exhausted cooking oils were evaluated for the production of OleoPlast. The resulting material, OleoPlast, was then ground to obtain pellets used to produce the samples characterized in this work. The pellets can be processed with various techniques and shapes, including filaments suitable for 3D printing and thin sheets, Fig. 1a. These sheets can be printed on using a standard inkjet printer, much like regular paper, as demonstrated by the printed University of Salento logo and the EC chemical formula. Differential scanning calorimetry (DSC) characterization was conducted to prove the thermoplastic nature of OleoPlast. In Fig. 1b, the DSC analysis between −30 and 180 °C of pure EC, oil, and OleoPlast with varying EC content, is presented. The EC exhibited a glass transition at ~135 °C, while the oil displayed a linear heat flow across the tested range, with a melting temperature centered at ~−5 °C. OleoPlast shows an endothermic/exothermic peak at a temperature of ~110 °C, indicating the melting and solidification of the materials, respectively. Significantly, the DSC analysis demonstrates the gel nature of OleoPlast, evidenced by the peaks corresponding to the fusion and solidification of the oil (<−5 °C), confirming the presence of oil in a liquid state in the OleoPlast, highlighting its gel-state at room temperature. Moreover, DSC analyses were performed on OleoPlast samples using various oils, including PEA, SB, SF and exhausted oil (Extended Data Fig. 1). The DSC analyses indicated no significant differences in the thermodynamic behavior of OleoPlast when different oils were used, except for the fusion and solidification temperatures of the oil itself, which depended on the varying content of saturated and unsaturated fatty acids. Table 1 details the average fatty acid composition of the different oils employed in the study [28–30]. The exact fatty acid profiles for each oil employed in the study are detailed in the Materials and Methods section. Within the analyzed range, OleoPlast displays remarkable stability, as evidenced by thermogravimetric analysis (TGA; details in Extended Data Fig. 2), where the degradation temperature was recorded above ~350 °C. This emphasizes a significant difference between the processing temperatures (<170 °C) and the degradation temperature, a desired characteristic in thermoplastics and often absent in biopolymers (e.g. PHB [31]).

A critical aspect of a thermoplastic material is its ease of adoption in large-scale manufacturing processes such as injection molding or extrusion. For this reason, it is crucial to assess the flow behavior of the material. Fig. 1c reports a temperature sweep rheological characterization was performed to highlight the crossover points of the material, marking the transition from a solid-like to a liquid-like behaviour [22,32] The storage modulus (G') and loss modulus (G'') of OleoPlast increase with the polymer concentration. At temperatures below 100 °C, G' consistently exceeds G'', indicating a predominantly elastic behavior. The crossover temperature, where G'' becomes greater than G', also rises with increasing polymer concentrations. Extended Data Fig. 3 reports the phase angle, highlighting the gel behavior of the material and the shift of the curve towards higher temperatures with increasing polymer content. These temperatures were found to range between 140 and 160 °C (Fig. 1d), showing minimal variations with the type of oil used and being primarily influenced by the polymer concentration in the OleoPlast. Defining these temperatures is essential for establishing the reprocessing conditions (e.g., injection molding, hot pressing, 3D printing) of OleoPlast, where its viscous behavior plays a critical role. An X-ray diffraction (XRD) analysis was conducted to assess the crystallinity of OleoPlast, revealing an amorphous-like structure (Fig. 1e). Notably,

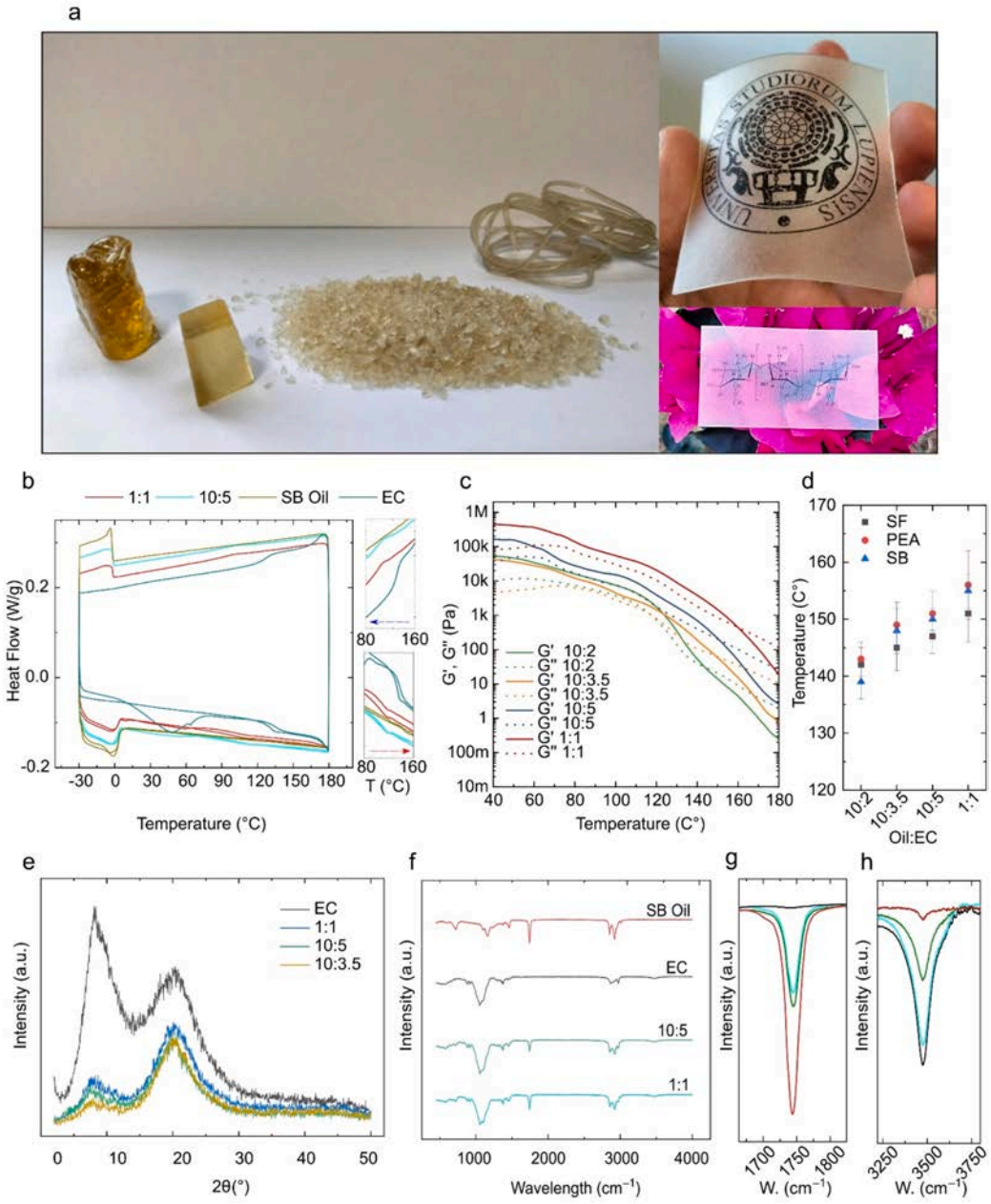

Fig. 1. a) picture of OleoPlast in different forms: pellets, casted forms, and extruded filament. On the side, OleoPlast film was utilized as a substrate to print the University logo and the chemical formula of Ethyl Cellulose; b) DSC characterization of EC, SB oil, and SB OleoPlast with varying polymer concentrations. Three ramp cycles were conducted: one from −30 °C to 180 °C, the second from 180 °C to −30 °C, and the third from −30 °C to 180 °C. On the side, zooms are reported to highlight the endothermic and exothermic peaks of fusion and solidification in OleoPlast; c) The figure shows the storage modulus (G') and loss modulus (G'') of OleoPlast at different polymer concentrations. The data indicates that both G' and G'' increase with higher polymer content. Initially, G' is greater than G'', signifying a predominantly elastic behavior. The crossover temperature, where G'' surpasses G', also rises with increasing polymer concentration. d)The temperature crossovers of OleoPlast, marking the transition from a solid-like to a liquid-like behavior; e) XRD analysis of EC and SB OleoPlasts with different polymer concentrations; f) FTIR fingerprint of SB OleoPlasts. g-h) show zoomed-in views and overlays of the peaks at 1745 cm^{-1} and 3477 cm^{-1}, which are characteristic of the ester groups in fatty acids of the oils and the hydroxyl groups in EC, respectively. These peaks align with the concentrations of oil and EC.

Table 1
Saturated Monounsaturated and polyunsaturated fatty acid average composition (%) of employed vegetable oils.

Oil	Saturated	Monounsaturated	Polyunsaturated
SF	9–13	25–33	55–65
SB	14–16	20–25	55–65
PEA	16–20	50–60	20–30

the peak at 10° associated with EC is strongly reduced in the OleoPlast due to the plasticizing effect of the oil within the polymer matrix (Extended Data Fig. 4 reports the XRD analysis on different OleoPlasts). In Fig. 1f, the FTIR analysis illustrates the chemical fingerprint of the material, showing a distinctive overlap of EC and oil spectra that characterizes the OleoPlast. Fig. 1g–h report specific peaks, particularly at ~1745 cm^{-1} corresponding to the ester groups in triglycerides [33] and at ~3477 cm^{-1} corresponding to the hydroxyl groups in cellulose [20,34]. As observed, OleoPlast formulations exhibit both peaks proportionally to the oil and polymer content, without significant frequency

shifts. This confirms that the oleogels are primarily structured by weak bonds such as van der Waals and hydrogen bonds [23]. A comprehensive FTIR characterization is reported in Extended Data Fig. 5.

The elongation at break, maximum sustained stress, and Young's modulus of OleoPlast were assessed through tensile testing. Injection molding was employed to process OleoPlasts, generating dog bone specimens (Extended Data Fig. 6). Stress–strain curves for different SB oil and EC ratios are shown in Fig. 2a. The values of the maximum sustained strain, stress, and Young's modulus are shown for all the pristine oils types (i.e. SF, PEA, SB), and oil-EC ratios (i.e. 10:2, 10:3.5, 10:5 and 1:1) in Fig. 2a (experimental details in the Materials and Methods section). In general, with the increase in polymer content, a rise in modulus and maximum sustained stress was observed, accompanied by a reduction in maximum sustained strain. Noteworthy, OleoPlast can own a wide range of Young modulus, spanning from ~2 MPa to ~250 MPa, emphasizing the significant tunability of its mechanical properties.

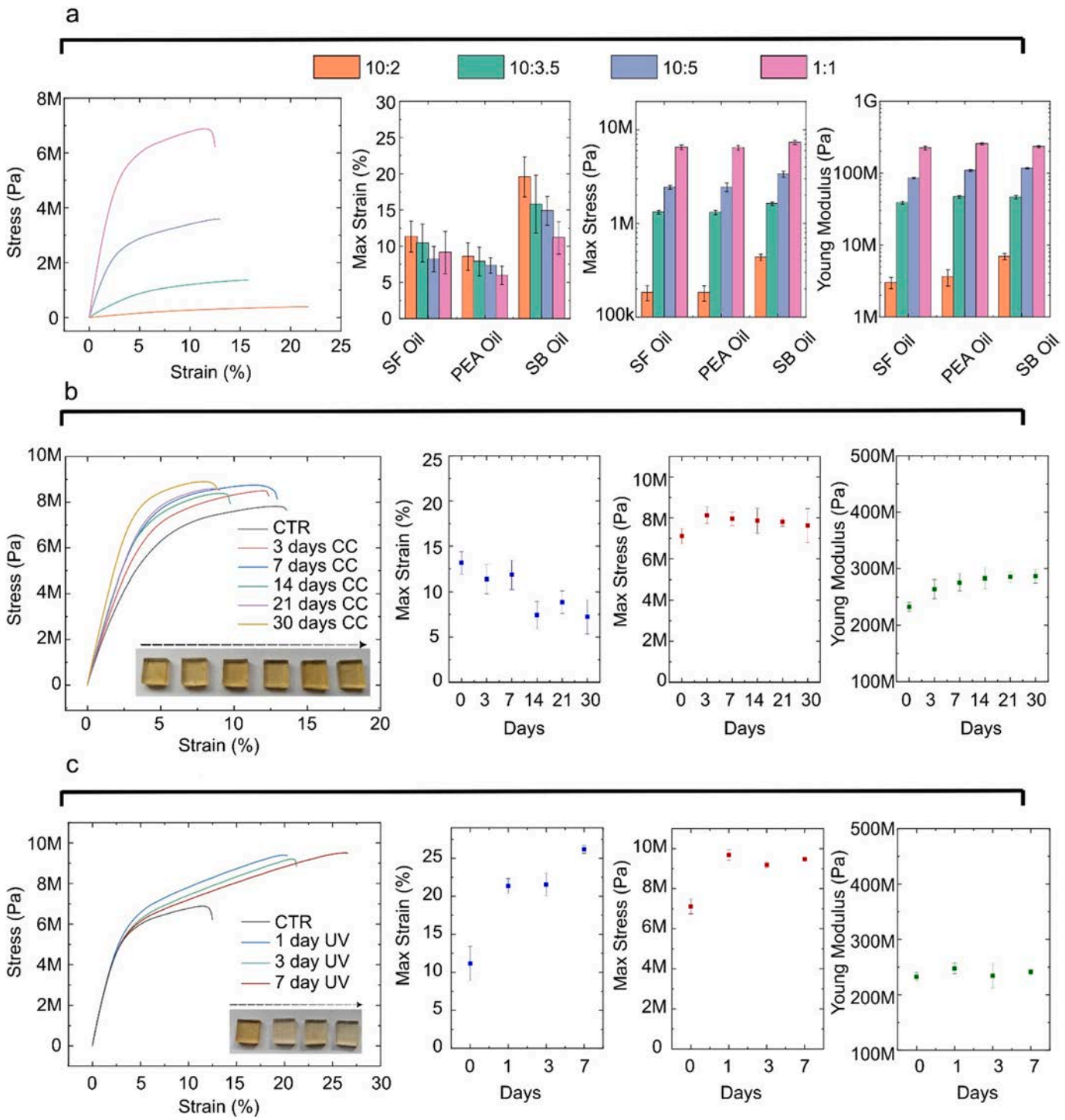

Fig. 2. a) stress–strain curves of SB Oil OleoPlast at different polymer oil concentrations and their respective elongation at break, maximum sustained stress, and Young's modulus; b) Stress–strain curves of SB OleoPlast 1:1 aged in a climatic chamber and the respective elongation at break, maximum sustained stress, and Young's modulus. The inset shows a picture of the OleoPlast at different time points; c) Stress–strain curves of UV-aged SB OleoPlast 1:1 and their respective elongation at break, maximum sustained stress, and Young's modulus. The inset displays a picture of the OleoPlast at different time points.

Interestingly, samples with SB oil exhibited superior stretchability, with an ~80 % average increase of maximum sustained strain with respect to other oils. This is attributed to the higher affinity of SB oil with the EC, which enhances chain mobility and improves the plasticity of the OleoPlast [32]. Each type of oil has distinct compositions of saturated, monounsaturated, and polyunsaturated fatty acids, significantly influencing the polymer matrix interaction [35]. It is plausible that further exploration or incorporation of different oils, fatty acids and their blends could finely tune and augment these characteristics. The utilization of different vegetable oils does not impact the water wettability of OleoPlast, which remains around 90° (Extended Data Fig. 7).

The study investigated the impact of increasing the polymer concentration to a 1:2 oil-to-EC ratio, assessing the maximum solubility of EC in oil. OleoPlast with this ratio exhibited an increase in Young's modulus, reaching approximately 500 MPa, and maximum sustained stress around 10 MPa, though extensibility decreased to less than 5 % compared to the 1:1 ratio, as shown in Extended Data Fig. 8. However, small benefits from higher polymer concentration were offset by longer solubilization times and potential cost increases. Additionally, the work evaluated the use of exhausted cooking oil, a common food industry by-product, in OleoPlast to test its compatibility with the production process. The use of such oil did not significantly affect the mechanical properties of OleoPlast in terms of Young's modulus, elongation at break, and maximum sustained stress, as illustrated in Extended Data Fig. 8. This demonstrates the adaptability of OleoPlast and its suitability for circular economy applications. However, since OleoPlast produced with the different oils exhibited similar mechanical properties, except for OleoPlast made with SB which displayed the highest elongation at break, subsequent characterizations were carried out using SB oil as the standard. Systematic use of exhausted oil was avoided to ensure the reliability of the study, as the formulation of such oil is inherently variable and can differ significantly from batch to batch.

One of the main problems of bioplastics is their poor stability to environmental conditions such as humidity, temperature, and UV light [36–39]. OleoPlast has been aged under harsh conditions in a climatic chamber and under UV exposure in order to assess its stability. Fig. 2b comprehensively illustrates the mechanical properties of OleoPlast after 3, 7, 14, 21, and 30 days of conditioning within a climatic chamber maintained at 90 % humidity and 40 °C. OleoPlast highlighted a decrease in its maximum strain (~40 % after 30 days) and an increase in its Young modulus (~20 % after 30 days). This process might be attributed to the recrystallization of EC, caused by the increased mobility of polymer chains within the gel during aging in the climatic chamber [40,41]. However, no significant change in the crystalline degree is observed, likely due to the high oil content in the material, as shown in Extended Data Fig. 9. Extended Data Fig. 10 reports a reduction in water contact angle likely linked to a segregation phenomenon concerning EC during the aging process. This segregation alters the surface dynamics, affecting the interaction between the material and water. Noteworthy, the samples kept at room temperature showed no change in the mechanical properties even after 3 months, Extended Data Fig. 11.

OleoPlast was subjected to a 7-day UV aging process, providing an equivalent of approximately 3.5 years of UV exposure (details in the methods section). Interestingly, the UV exposure positively affects the plastic field deformation of the material increasing the maximum sustained stress (+35 %) and doubling the stretchability of OleoPlast, Fig. 2c. The change in mechanical properties is primarily due to the chemical modifications of OleoPlast, as observed in the FTIR in Extended Data Fig. 12. UV exposure leads to the formation of epoxides on the double bonds of the fatty acids in SB oil and to transesterification reactions between these and the cellulose [42,43]. Additionally, UV exposure resulted in a bleaching effect on the OleoPlast, as visibly depicted in the inset picture, confirming alterations at a molecular level [44]. The UV exposure does not affect the water contact angle Extended Data Fig. 13.

Importantly, no additives (e.g. plasticizers, thermal stabilizers, radical inhibitors, UV stabilizers, antioxidants) were introduced to assess the intrinsic mechanical properties and stability of the OleoPlast under challenging environmental conditions, representing a foundational stage that can be further enhanced with potential additives in the future.

The end-of-life management of plastics is an enduring challenge. Many plastics encounter difficulties in terms of reusability and recyclability due to molecular degradation and the prevalent use of additives in finished products [45,46]. The recycling processes tend to be detrimental to plastics, whether they are petroleum-based or bio-based. This results in substantial declines in their mechanical properties [10,47–49]. For instance, PET experiences a reduction of over 75 % in elongation at break and more than 50 % in tensile strength after undergoing five recycling cycles [50]. Similarly, Polylactic acid (PLA), a widely produced biopolymer globally, can only be recycled a few times, as its physical properties, including stress and strain at break, consistently decrease by more than 40 % after five recycling cycles [13,51]. OleoPlast displays significant mechanical recyclability, successfully withstanding up to 5 recycling cycles, Fig. 3a. During this process, OleoPlast has shown only a minor reduction in maximum sustained stress (~5%) associated with a darkening of the material. Notably, Young's modulus and elongation at break remained consistently stable as well as the water contact angle (Extended Data Fig. 14). The notable recyclability potential of OleoPlast is linked to two key factors: i) its gel state nature, being 50 % polymer, results in lower polymeric degradation during mechanical recycling processes; ii) the notable difference between its processing and degradation temperature ($\Delta T > 100$ °C), as evidenced by DSC and TGA studies. These findings emphasize the promising potential for material reusability, highlighting its capacity to significantly contribute to a sustainable circular economy.

Unfortunately, even though recycling is the preferable route for a circular economy, a considerable amount of plastic ends up dispersed in the environment, particularly in the oceans, leading to severe environmental impacts [9]. As such, recyclability does not suffice, and a high degree of biodegradation in the environment is necessary to ensure sustainability. An assessment of OleoPlast biodegradation in seawater was therefore conducted, adopting a Biochemical Oxygen Demand (BOD) analysis for a 30-day period [52]. The biodegradation process starts after 3 days in seawater and progresses until the end of the experiment (Extended Data Fig. 15 for detail). In Fig. 3b, the final BOD values of OleoPlasts are compared with those of other common bioplastics. OleoPlast exhibited notable biodegradation, with a final BOD comparable to that of polyhydroxybutyrate (PHB), a widely recognized biodegradable bioplastic [53].

The solubility and stability assessment of OleoPlast in the most common organic solvents, water, and a phosphate buffer saline (PBS) solution was evaluated. This characterization defines the reprocessability of OleoPlast via solvent-based methods, paving the way for applications like solvent casting and thin coating. Simultaneously, it explores the recovery potential of OleoPlast components—EC and oil—enabling integration into new supply chains. This approach aligned with sustainability goals promotes the circular use of OleoPlast constituents in different industrial processes. OleoPlast demonstrated high solubility in nearly all pure organic solvents, but not in water and PBS, in which it exhibited stability for over 10 days, Extended Data Fig. 16. Realistically, plastics rarely encounter pure solvents in typical use cases. The OleoPlast stability in diluted solvent solutions of 80 % and 50 % has been evaluated, Fig. 3c and d. In the 80 % diluted solutions, OleoPlast dissolved within a day in THF and alcoholic solutions, within 3 days in an acetic acid solution, and displayed swelling when exposed to acetone. On the contrary, at a 50 % dilution, the material remained stable in all organic solutions except THF, Extended Data Fig. 17. The results highlight how OleoPlast could be incorporated and reprocessed in different industrial streams through the use of organic solvents while remaining compatible with common applications.

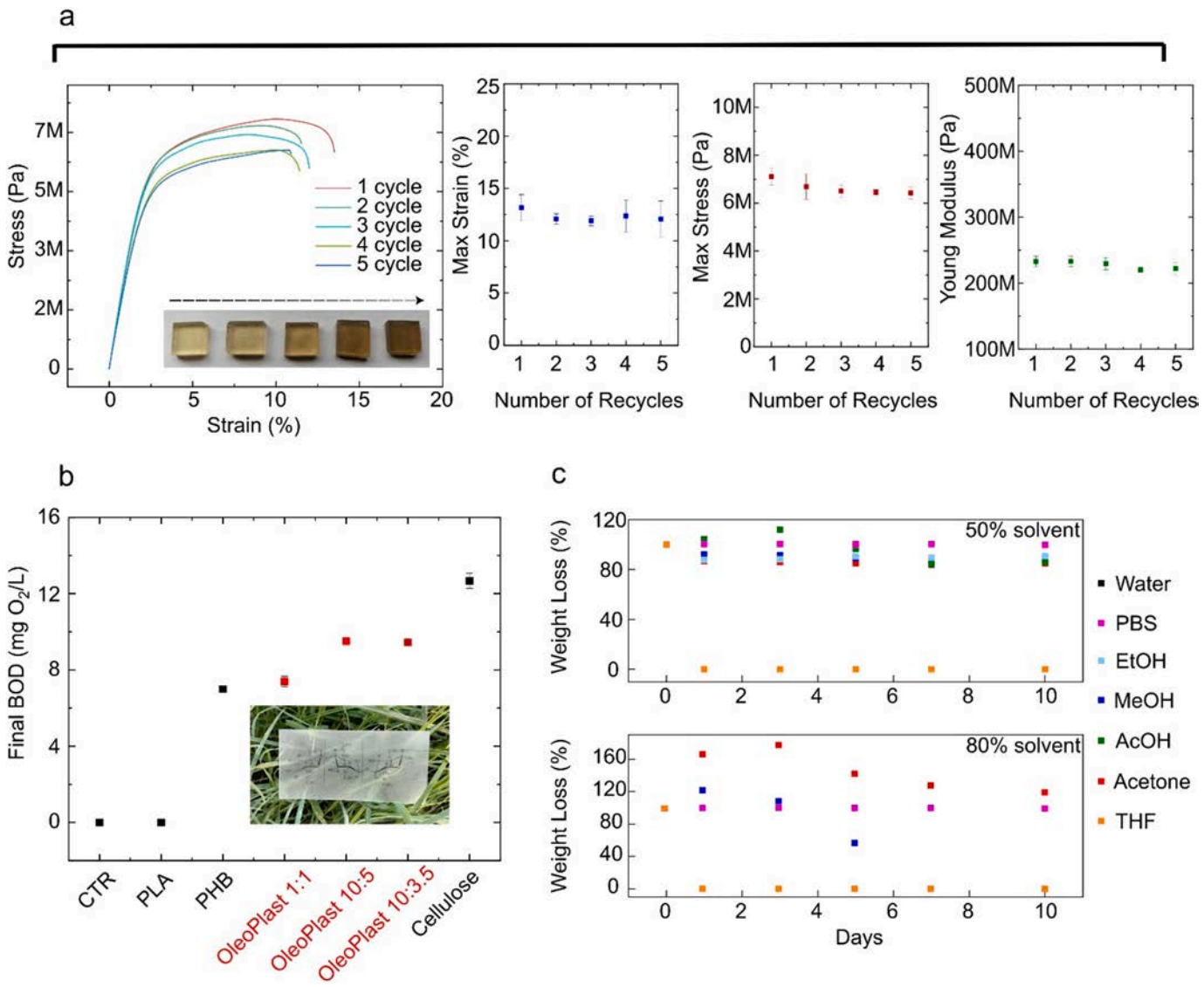

Fig. 3. a) stress–strain curves of recycled OleoPlast and their respective elongation at break, maximum sustained stress, and Young's modulus. The inset displays pictures of the OleoPlast after each recycling cycle; b) Final Biological Oxygen Demand (BOD) of OleoPlasts and a comparison with other plastics, CTR is represented by the empty bottle. A picture of OleoPlast placed on green grass in the inset.; c) Solvent stability of OleoPlast in different solvents at 50% and 80%.

One of the most promising applications of OleoPlast is in food packaging, which represents approximately 40 % of the total plastic usage. However, plastic currently adopted in food packaging has a very short lifespan ranging from days to months, representing the first source of plastic pollution [7,54]. OleoPlast is made by EC (authorized by the European Food Safety Authority with E number 462) and vegetable oil, both approved for human consumption, which makes oleogels inherently suitable for food contact applications and potentially as edible food packaging [55]. Oxygen and water vapor transport rates (Fig. 4a and b) and UV–vis transmittance (Fig. 4c), key properties for food packaging film development, were assessed for various OleoPlast formulations. A lower permeability has been observed in OleoPlast with higher polymer content, suggesting that the polymer plays a role in enhancing the gas barrier properties. Concerning oxygen transmission rate (OTR), OleoPlast showed comparable levels to low-density polyethylene (LDPE) and cellulose acetate (CA), ~5k ml/m^2/day. In terms of water vapor transmission rates (WVTR), the values fell within the range of the most common bioplastics used in packaging: PLA, Polyhydroxyalkanoates (PHA), and Polycaprolactone (PCL), ~400 ml/m^2/day. Food products typically require also protection from UV light exposure, as it induces or accelerates degradation [56]. OleoPlast favorably shows a remarkably high absorbance in terms of UV light (<380 nm), as shown in Fig. 4c. The ability to directly print onto the surface, as illustrated in Fig. 1a, introduces an attractive additional food-packaging feature, which could enable the direct printing of food labels onto OleoPlast without the need for additional layers or films, improving sustainability and recyclability of the material.

Another pivotal and rapidly expanding market that necessitates sustainable and biodegradable plastic substrates is electronics, in demand of effective tools to tackle the electronic waste management problem [51]. OleoPlast, with inherent mechanical tunability, recyclability, biodegradability, and edibility, can emerge as a substrate of choice for growing sectors such as green electronics, flexible electronics, and even edible electronics [57–61]. In this regard, the dielectric properties of OleoPlast have been assessed, revealing a dielectric constant (ε_r) spanning from 2.7 to 3.1 and a loss tangent (tan δ) of approximately 0.05 in the frequency range 1.5–3.5 GHz [62] (Fig. 4d and e). Notably, these properties remained stable across various oil types, with only a slight reduction in ε_r observed in OleoPlast with lower polymer content. These values align precisely with those of polydimethylsiloxane (PDMS) and polyimide (e.g. Kapton), which currently stands as a gold standard in soft and flexible electronics [63,64]. To

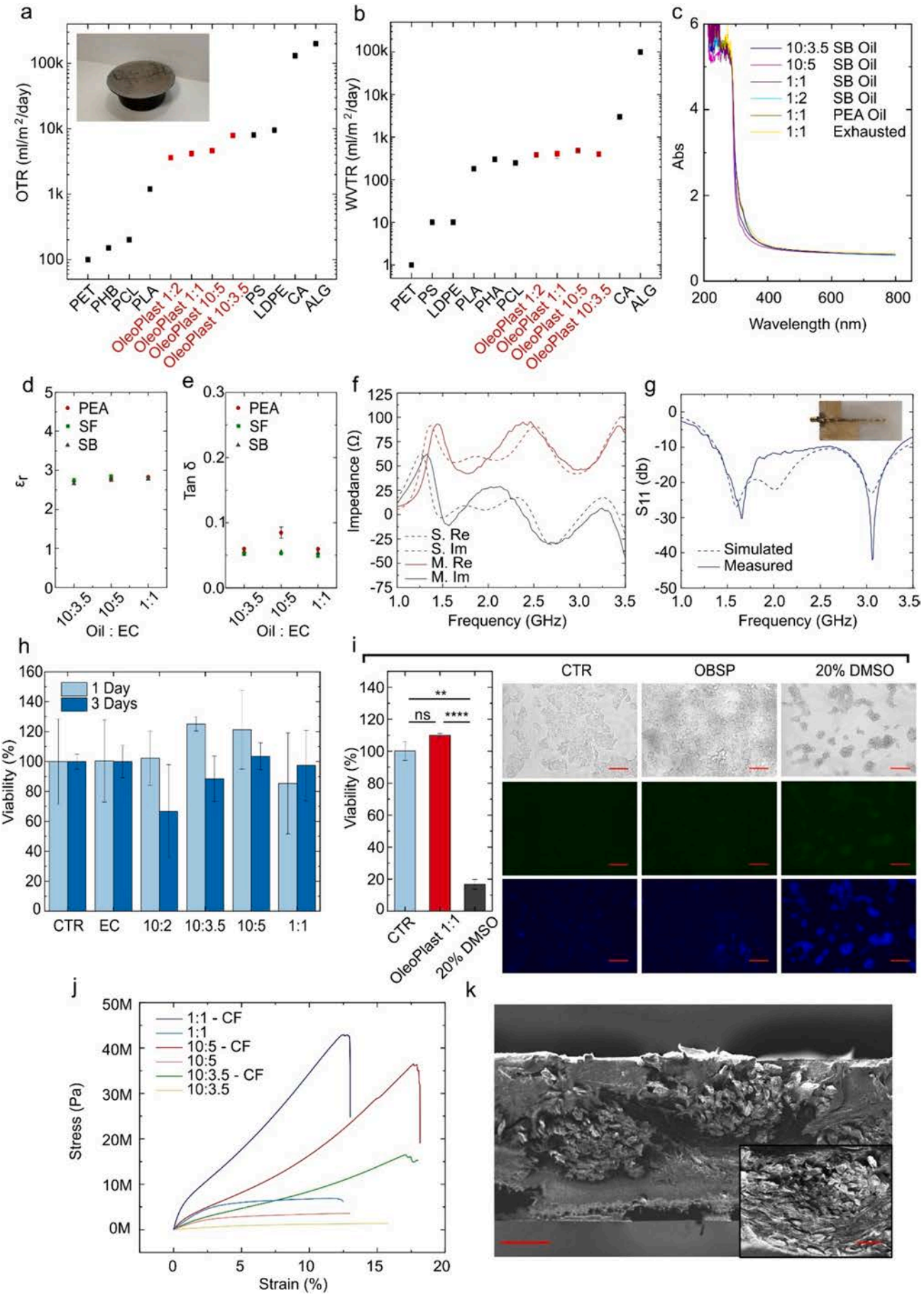

(caption on next page)

Fig. 4. a-b)Oxygen transmission rate (OTR) and water vapor transmission rate (WVTR), compared with common polymers, respectively. A picture of a coffee capsule coated with OleoPlast in the inset.; c) UV–Vis absorbance of OleoPlasts obtained with different polymer concentrations and oils; d-e) Dielectric constant (ε_r) and loss tangent (tan δ) of OleoPlast obtained with different polymer concentrations and oils; f) Measured and simulated impedance of the developed antenna; g) Measured and simulated reflection scattering parameter S_{11} of the OleoPlast antenna. A picture of the developed antenna in the inset; h) Quantification of HepG2 cell viability in different incubation groups, non-contact mode; i) On the left, quantification of HepG2 cell viability in different incubation groups, in-contact mode. On the right, bright-field, live/dead (green), and DAPI (blue) fluorescent images of the same cell groups. (* $p < 0.05$, ** $p < 0.01$, *** $p < 0.001$, **** $p < 0.0001$); j) Comparison of stress–strain curves among OleoPlasts and cotton fabric-OleoPlast composites; k) SEM cross-section of OleoPlast 1:1 – Cotton fabric (scale bar 100 μm), inset details the fiber impregnation (scale bar: 50 μm).

demonstrate the potential of OleoPlast as a dielectric component in electromagnetic devices, a proof of concept of a wide-band monopole antenna with circular polarization has been redesigned for the OleoPlast substrate [65]. The resonance of the antenna, realized using an edible gold leaf as electrode, was tuned within the frequency range spanning from 1.5 GHz to 3 GHz [65], a bandwidth encompassing communication technologies such as WiFi, Bluetooth, GPS, etc. Simulation results, performed using the tool CST Microwave Studio [66], displayed a good match with the experimental impedance data (Fig. 4f). The reflection scattering parameter S_{11} below −10 dB indicates efficient electromagnetic coupling in terms of impedance and maximum power transfer with a 50 Ω reference port [67], Fig. 4g.

Biocompatibility of alternative thermoplastics is of paramount importance, given the increasing demand for sustainable materials serving emerging applications such as implantable and wearable devices and drug release systems, as well as systems for tissue engineering. Biocompatibility of OleoPlast was preliminary assessed using the immortalized human hepatocarcinoma cell line HepG2, commonly employed as a model for investigating cytotoxicity, metabolism, and drug release systems [68,69]. OleoPlast exhibits excellent biocompatibility according to non-contact [70,71] MTT assays, (Fig. 4h), demonstrating no release of toxic compounds into the medium, regardless of the polymer concentration and the type of oil used (Extended Data Fig. 18). After confirming the non-contact biocompatibility of OleoPlast, a comprehensive assessment of its biocompatibility was undertaken through in-contact testing [72], which encompassed a morphological, live/dead (green) and DAPI (blue) fluorescent analysis. Notably, both bright-field and fluorescent staining images revealed regular cell morphology in both control and OleoPlast groups. On the contrary, the positive control group (20 % Dimethyl sulfoxide – DMSO) showed severe cell death as indicated by the bright blue color typical of apoptotic nuclei using DAPI staining, Fig. 4i. MTT assays further confirmed the results obtained, indicating high cell viability with no significant differences compared to the control group.

Bioplastics can play a key role also in the highly demanded and emerging field of sustainable composites, exploiting renewable and waste products to produce alternatives to composites made from resins and inorganic fibers, posing challenging waste management issues [73,74]. Fig. 4j and k illustrates the mechanical properties and SEM cross-section of a cotton fabric (CF) impregnated with the OleoPlast through compression molding, obtaining a fiber-reinforced composite. The stress–strain curve shows a remarkable enhancement in material properties, triplicating the modulus to ~700 MPa and increasing ~5 times the breaking load to ~40 MPa, with respect to the pristine OleoPlast (Extended Data Fig. 19 reports the complete characterization). The impregnation is efficiently performed resulting in a defect-free and homogeneous fiber-OleoPlast interface, which leads to the aforementioned reinforcement, as can be appreciated in the SEM images in Fig. 4k. The demonstrated capability to develop OleoPlast-based composites could pave the way for a broad range of biobased and biodegradable composite materials utilizing different matrices and fiber combinations.

The processability of bioplastics, especially those derived from cellulose, has long been a significant challenge due to their thermal and mechanical degradation, along with the need for solvents or plasticizers [10,15,20]. OleoPlast, however, shows remarkable versatility in this regard, showing compatibility with various prevalent large-scale and high-resolution industrial and laboratory manufacturing techniques, all achieved without the use of any solvent. In addition to the conventional thermoplastics production process of injection molding and hot pressing adopted to fabricate the samples under test in the previous experiments, OlePlast compatibility with more refined techniques was tested, CNC milling, micro compression molding, and 3D printing.

Fig. 5a shows pictures of "LEGO" like pieces produced through milling. The process yields a smooth finish, enabling a good fit between the pieces. Notably, the process avoids material overheating and fusion, a common occurrence with plastics (e.g. PLA). Furthermore, micropatterning capability of OleoPlast has been demonstrated through compression molding, producing a replica of an Arundo donax leaf (Fig. 5b and c), wherein structures of a few microns, such as stomata [75], can be appreciated in the inset. This property positions the material as a potential new platform for bio-soft robotics and microfluidics, presenting itself as a sustainable thermoplastic alternative to PDMS, which currently stands as a preferred choice in these fields. OleoPlast has also been extruded to produce a standard 1.75 mm filament (Fig. 5d), specifically for utilization in Fused Filament Fabrication (FFF) 3D printing. This enabled the prototyping of a simple porous scaffold with details as fine as 300 μm (Fig. 5e). These results mark a significant milestone, introducing a new bio-based, biodegradable, biocompatible, and even edible material into the field of 3D printing, offering OleoPlast as a novel platform material, an alternative to petroleum-based plastics and PLA, in the rapid prototyping for both academics and industry.

3. Conclusion and perspectives

OleoPlasts, namely ethyl cellulose-based oleogels, were introduced as a gel-state sustainable bioplastic platform. OleoPlast stands out as a versatile gel-state bioplastic, offering tunable mechanical, electrical and biocompatible properties, showing stability in harsh environmental conditions and holding high potential for a broad range of applications. It exhibits exceptional processability across large-scale and high-resolution manufacturing processing, including injection molding, 3D printing, CNC milling, and micro-compression molding. The exceptional tunability of OleoPlasts in mechanical properties, ranging from ~2 MPa to ~600 MPa, and their capability to form fiber-based reinforced composites, with Proof-of-concept prototypes in fields as diverse as structural composites, food packaging, green electronics, and tissue engineering, demonstrate OleoPlast potential in several sectors necessitating a transition to sustainable approaches. The possibility to incorporate exhausted oils and the notable stability of properties upon reuse further emphasize the alignment of OleoPlast with the principles of a circular and green economy.

The remarkable thermoplastic properties of OleoPlast, which achieves an unprecedented trade-off with biodegradability in seawater with the combination of vegetable oil and EC, mark the starting point of a broad field of research. In the future, further explorations will involve additional oils, not necessarily of vegetable origin, to modulate both biodegradability and mechanical properties. To clearly position OleoPlast within the plastic landscape, Table 2 provides a comparison of keys OleoPlast mechanical and physical properties with LDPE, the prevalent petroleum-based plastic, and PLA, a prominent biobased alternative.

This work demonstrates the use of oleogels, currently predominantly employed in food science, in applications previously unexplored in the realm of materials science. In the future, the OleoPlast concept can be widely extended, by studying the incorporation of additional molecules

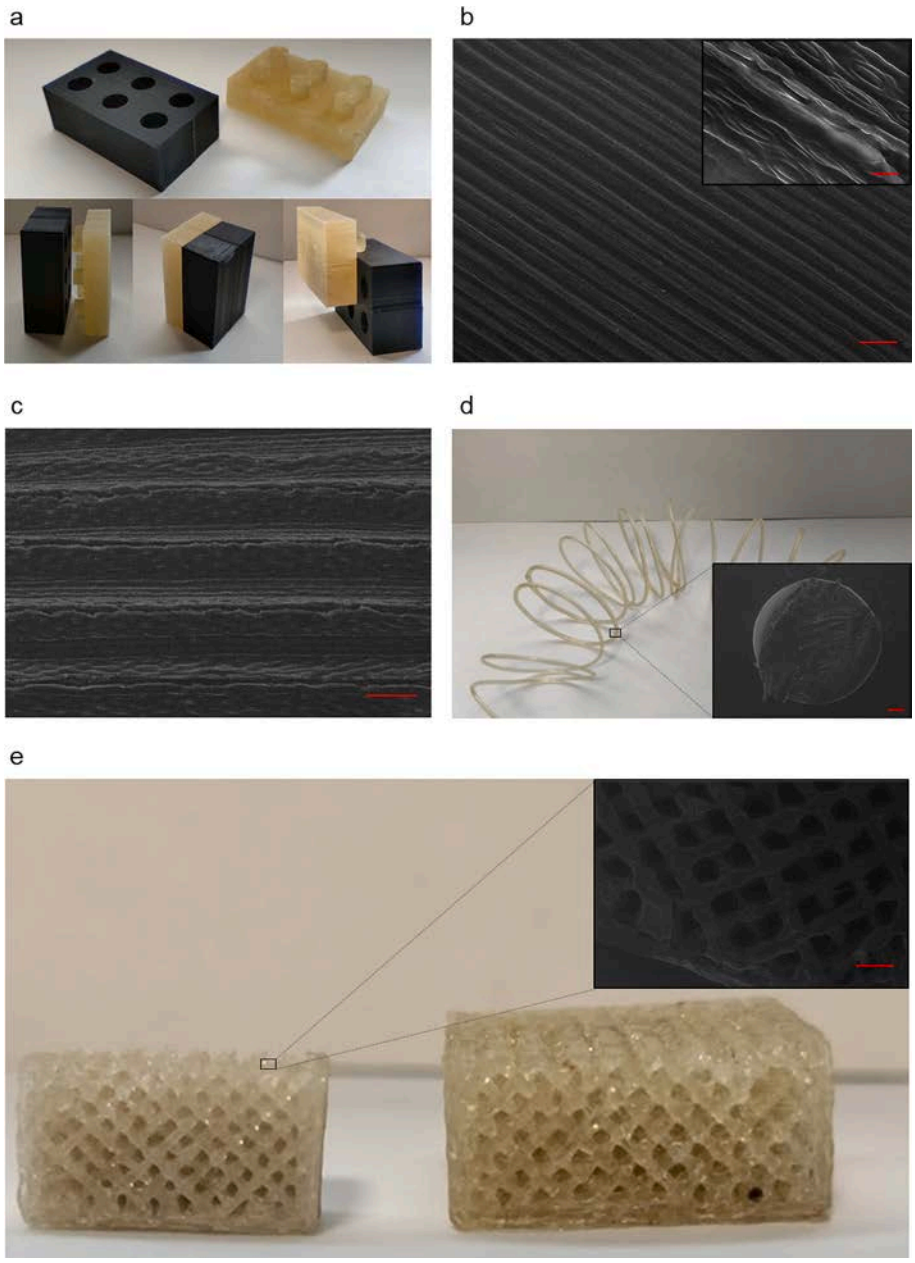

Fig. 5. a) the 1:1 OleoPlast has been processed with CNC to fabricate LEGO-like structures. The dark coloration was achieved by incorporating 0.1 % w/w Oil Blue into the OleoPlast; b) SEM image of an OleoPlast-replicated Arundo donax leaf using compression molding (scale bar: 400 μm). Inset highlights microstructure details of stomata (scale bar: 20 μm); c) SEM image of the same microstructure tilted at a 45° angle, highlighting the 3D pattern of the leaf (scale bar: 100 μm); d) Extruded 1:1 OleoPlast filament with a 1.75 mm diameter, along with a cross-section detail provided in the inset (scale bar: 100 μm); e) 3D-printed 1:1 OleoPlast scaffold with details of approximately 300 μm and 400 μm, from left to right respectively. SEM image of the scaffold with a detail of ~300 μm in the inset (scale bar: 1 mm).

Table 2
Comparison of OleoPlast mechanical and physical properties with LDPE and PLA.

	LDPE	PLA	OleoPlast
Bio-based	No	Yes	Yes
Melting temperature (°C)	~110	~180	~150
Degradation temperature (°C)	~390	~290	~350
Young Modulus (GPa)	0.1–0.4	1–3	0.003–0.6
Elongation at break (%)	200–500	2–5	20–25
Biodegradation in seawater	No	No	Yes
Recyclability	Yes	Poor	Yes
OTR ($ml/m^2/day$)	~5k	~1k	~5k
WVTR ($ml/m^2/day$)	~10	~200	~400

such as free fatty acids, waxes, stabilizers, plasticizers, synthetic oils and chemical crosslinking agents. Concerning packaging, barrier properties can be tuned and improved with the addition of free fatty acids and waxes that have already proven their barrier capabilities [76,77]; moreover, the development of phase-changing food packaging that exploits the gel state of OleoPlast can be envisioned [78]. In electronics, OleoPlast has the potential to offer powerful new opportunities within the emerging domains of organic, green and even edible electronics. Both dielectric and conductive properties could be modified in OleoPlast through the addition of salts, ceramics, or conductive fillers (e.g., carbon-based or metallic), paving the way for 3D- OleoPlast printable electronics. Furthermore, the possibility to micropattern the OleoPlast will open the door to new microfluidics systems based on OleoPlast. In tissue engineering, OleoPlast could represent a game changer in the

development of 3D-printable systems for tissue engineering that can be easily modified by researchers and clinical requests. This is facilitated by the gel state of OleoPlast, allowing for the addition of bioactive proteins or ceramics.

This foundational work sets the stage for further tailoring and customization of a sustainable bioplastic system, paving the way for the evolution of this material platform to meet the evolving demands of sustainable scientific and industrial landscapes, spanning from packaging to electronics and tissue engineering. Looking forward, the vast potential of OleoPlast holds exciting prospects for the development of innovative, eco-friendly solutions across different domains.

4. Materials and methods

4.1. Materials

Ethylcellulose (48–49.5 w/w ethoxyl basis), Oil Blue, and all the solvents were bought from Sigma Aldrich. Vegetable Oils (Peanuts, Soybean, and Sunflower) were bought in a supermarket. Specifically, we chose Desantis brand oil. The peanut oil contains 19 % saturated fatty acids, 53 % monounsaturated fatty acids, and 28 % polyunsaturated fatty acids. The soybean oil contains 15 % saturated fatty acids, 24 % monounsaturated fatty acids, and 61 % polyunsaturated fatty acids. The sunflower oil contains 12 % saturated fatty acids, 32 % monounsaturated fatty acids, and 56 % polyunsaturated fatty acids. Edible gold leaf was bought from Kinno (thickness < 500 nm). Exhausted oil, kindly provided by local fast food, was used after being filtered using a paper-based method to remove solid particles. Plain-woven and bleached 100 % cotton fabric, with 180 ± 5 g/m^2 mass density, was purchased from a market for use in the experiments. The fabric has a thread density of 24 threads/cm in both the warp and weft directions.

4.2. Methods

4.2.1. OleoPlast production

OleoPlast was produced via hot mixing at 165 °C. In general, oleogels form at temperatures above the glass transition temperature (of EC, approximately 135 °C, as confirmed by DSC (Fig. 1b). The optimal mixing temperature for our setup was determined to be 165 °C, which is around 10 °C above the crossover temperature observed in rheological analyses (Fig. 1b and c). This temperature ensures a significant reduction in viscosity by about three orders of magnitude, as estimated by the Williams-Landel-Ferry equations, facilitating efficient material mixing.

In the production process, the oil was heated to 165 °C while stirring at 50 RPM. EC was gradually introduced to the heated oil to prevent clumping and ensure uniform incorporation. Once all EC was added, the mixture was maintained at temperature until a clear solution was achieved, indicating complete dissolution. The dissolution times varied depending on the polymer concentration: formulations with a 10:3.5 and 10:5 ratio required 30 to 40 min, the 1:1 ratio formulation needed about 60 min, and the 2:1 ratio formulation, due to its higher viscosity, required approximately 120 min.

Following mixing, the material was allowed to cool to room temperature and then frozen at −20 °C. This freezing step is essential for facilitating subsequent grinding, which was carried out using a vertical mill.

4.2.2. Injection molding

The ASTM D638 Type V specimens were fabricated using Injection molding (BOY Machine XS). Specifically, the feeding chamber was set to a temperature of 160 °C, the central chamber to 150 °C, and the nozzle to 135 °C. The injection pressure was maintained at 20 bar, the holding pressure at 15 bar, and the plasticization pressure at 1 bar.

4.2.3. Extrusion

The extrusions were conducted using the Felfil Evo Filament Extruder at a temperature of ~130 °C to obtain a uniform filament with a diameter of 1.75 mm.

4.2.4. CNC and 3D printing

Computer numerical control (CNC) and Fused Filament Fabrication (FFF) printing were conducted using a Creality CP01. Specifically, CNC operations were performed using a 3 mm diameter cutting tool, while 3D printing was conducted at a temperature of ~140 °C, utilizing nozzles with diameters of 0.3 mm and 0.4 mm.

4.2.5. Compression molding

Compression molding was carried out with a hot press at 165 °C. The master employed in this procedure was a freshly harvested leaf of Arundo donax.

4.2.6. DSC

DSC analysis was carried out using a DSC Q2500 (TA Instruments). Samples weighing 20.0 ± 1 mg were securely sealed in aluminum pans and subjected to a series of heating and cooling cycles. Each sample underwent heating from −30 °C to 180 °C at a rate of 5 °C/min, followed by cooling to −30 °C at the same rate, and then heating again to 180 °C at 5 °C/min. An empty aluminum pan served as the reference.

4.2.7. TGA

TGA analysis was conducted using a TGA Q500 instrument manufactured by TA Instruments with aluminum pans. Measurements were conducted using 3–5 mg of the samples, which were placed in an aluminum pan and exposed to a flow of inert N_2 gas at a rate of 50 mL/min. The pan underwent heating from 0 to 800 °C at a rate of 10 °C/min. The recording of weight loss was performed, tracking its variation over time and temperature.

4.2.8. Rheology

The rheological temperature tests were conducted using a parallel plate rheometer (Malvern Kinexus Pro + -Worcestershire, UK) on 1 mm thick films of OleoPlast. The tests were performed in a temperature range from 40 °C to 180 °C, with a controlled ramp rate of 5 °C per minute at frequency of 1 Hz and amplitude of 0.1 %. During these tests, both the elastic shear modulus G' and the viscous shear modulus, G'' have been recorded.

4.2.9. XRD

The crystallinity of OleoPlast and EC was analyzed using X-ray diffraction (XRD) technique. The measurements were conducted with a Rigaku Ultima X-ray diffractometer (Rigaku, Tokyo, Japan), employing monochromatic Cu Kα radiation ($\lambda = 0.154$ nm) at an operating voltage of 40 kV and current of 20 mA. Diffractograms were recorded at a scanning rate of 0.02° min^{-1} within the angle range of 2° to 50°.

4.2.10. FTIR

FTIR measurements were conducted using a Perkin Elmer Spectrum instrument (Waltham, USA) within the spectral range of 4000–500 cm^{-1}, employing a resolution of 0.1 cm^{-1}.

4.2.11. Stress–strain

The mechanical properties were evaluated at room temperature through uniaxial tensile testing utilizing a Zwick/Roell universal testing machine (Ulm, Germany) and employing dogbone-shaped ASTM D638 Type V specimens. A testing velocity of 5 mm/s was utilized for the assessments. Each measurement was performed in triplicate, and an average value was calculated for analysis.

4.2.12. Aging climatic chamber

The aging experiments in controlled temperature and humidity conditions were conducted in a Binder climatic chamber set at 40 °C and 90 % relative humidity (RH) for 30 days.

4.2.13. Aging UV

The UV lamp power was calculated using CR10 radiometer, yielding UV-A and UV-B values of 0.6 and 0.73 W/m^2 at 340 and 310 nm, respectively. This translates to daily energy levels of 52 and 63 kWh/m^2. Extrapolating to an annual UV exposure of approximately 100 kWh/m^2, constituting 10 % of the total solar UV radiation on Earth, the 7-day aging in this study simulates about 3.5 years of UV exposure.

4.2.14. Contact angle

The contact angle of OleoPlasts was measured using the sessile drop method at room temperature. In this method, a droplet of water was carefully placed on the surface of the OleoPlast film. The static contact angle, which is the angle at which the droplet meets the surface, was measured. This was done using First Ten Angstroms, FTA 1000 software (Newark, California, USA) equipped with a CDD camera.

4.2.15. SEM

The morphological characterization of OleoPlast was performed by Zeiss Field-emission Scanning Electron Microscope (FESEM), (Sigma VP, Carl Zeiss, Jena, Germany) with an accelerating voltage of 10 kV. The morphological analysis of (CF)-OleoPlast was carried out using a JEOL JSM-6490LA SEM microscope. The cross-sectional samples were subjected to immersion in liquid nitrogen followed by fracturing. These fractured samples were affixed to aluminum stubs using carbon tape and coated with a 10 nm layer of carbon through sputter coating. Micrographs were captured at various magnifications, employing a 5 kV accelerating voltage and a load current of 78 μA.

4.2.16. Recycling

Mechanical recycling involved grinding the OleoPlast, followed by thermoforming using the injection molding process.

4.2.17. BOD

We investigated the biodegradation in water by assessing the biochemical oxygen demand (BOD) using the OxiTop-IDS system. Oxygen consumption was observed in a sealed bottle containing 432 mL of seawater, serving as the sole carbon source, along with a small quantity of each sample. The experiments were conducted at room temperature using dark glass bottles hermetically sealed with the OxiTop measuring head. Sodium hydroxide was used as a CO_2 scavenger to capture carbon dioxide generated during biodegradation. The biotic consumption of oxygen in the bottles' free volume was recorded based on the pressure decrease. Raw data of oxygen consumption (mg O_2/L) were analyzed by subtracting the mean values of the blanks, determined by measuring the oxygen consumption of seawater without any test samples. Following this correction, the values were normalized to the mass of the individual samples and expressed as mg O_2/100 mg of a sample.

4.2.18. Solubility

The chemical solubility of OleoPlasts was evaluated in 50 % and 80 % solutions of the following solvents: water, PBS, ethanol, methanol, acetone, tetrahydrofuran, and acetic acid. For this purpose, 1 cm^2 squared specimens were cut and immersed in 10 mL of solution. The dimensions and weight were measured for up to 10 days. The experiment was conducted in triplicate.

4.2.19. Composite development

The composite material (CF)- OleoPlast was obtained via compression molding within a 10 × 10 cm^2 frame with a thickness of 200 mm. 2.2 g of OleoPlast pellets were distributed below and above a layer of cotton fabric, cut to fit the 10 x 10 frame, the ensemble was molded between thin Teflon sheets at a temperature of 165 °C using a CARVER 4122 hydraulic press [51]. The molding sequence included a 5-minute heating phase without applying pressure, followed by an additional 5 min under a load of 4 tons and subsequent water cooling.

4.2.20. Gas barrier properties

The gas barrier properties of OleoPlast were assessed through measurements of water vapor permeability (WVP) and oxygen permeability (O_2P). To determine WVP, aluminum-based permeation capsules (7 mm inner diameter and 10 mm inner depth) were filled with 350 μL Milli-Q water, creating a humid environment (100 % RH). These capsules were sealed on top with the OleoPlast samples using two O-rings and a ring-shaped lid secured with screws. The analysis was conducted in triplicate for all samples. The sealed capsules were stored in a chamber at 0 % RH, simulated with dried silica gel. The weight of the capsules was monitored over time. The weight loss (g) of the capsules against time (s) was plotted, and the slope obtained after linear fitting was divided by the exposed film area (m^2) to determine the water vapor transmission rate (WVTR). To obtain the WVP (g m^{-1} s^{-1} Pa^{-1}) was employed the formula $WVP = WVTR \times t/PH_2O \times \Delta RH$. t is the mean thickness of each sample (m), PH_2O (Pa) is the vapor pressure of water at saturation and testing temperature (20 °C), and ΔRH is the variation in vapor pressure across the film. The measurement of O_2P for the OleoPlast was conducted using an Oxysense 5250i instrument (Oxysense, USA), equipped with a film permeation chamber. This chamber comprises a cylinder divided in two parts: a measurement well and a drive well. The sensing well contains a fluorescent sensor, the OxyDot, sensitive to oxygen concentration. The sensing well is purged with nitrogen while the driving well is exposed to the environment. Rectangular pieces of the films (6 cm × 6 cm) are placed in the chamber to separate the two wells. A fiber optic OxySense pen measures oxygen from the OxyDot at specific intervals. The oxygen transmission rate (OTR), defined as the volumetric flow rate of oxygen per unit area of film per unit time (mL m^{-2} day^{-1}), is measured by the instrument until a steady state is achieved. The oxygen permeability (O2P) of the films is then calculated using the following formula: O2P (mL μm m^{-2} day^{-1} atm^{-1}) = OTR. t/ ΔP, where t is the film thickness (μm), and ΔP is the partial pressure of oxygen (1 atm). All tests were conducted under ambient conditions (23 °C and 50 % relative humidity) following the ASTM method F3136-15 [79].

4.2.21. UV–vis

The absorbance of OleoPlast was experimentally evaluated using a Cary 6000i UV–Vis-NIR spectrophotometer (Agilent Technologies, USA) in the range of 210–800 nm. The reported data corresponds to the absorbance of a 500 μm film obtained through hot pressing.

4.2.22. RF characterization

To evaluate the dielectric constant (ε_r), and the loss tangent (tanδ) of the materials under test, the method of the T-Resonator has been used and properly implemented according to the methodology proposed in [80]. This last consists in a two-port microwave circuit that has a microstrip line with an open-ended stub resonating at odd-integer multiples of its quarter-wavelength corresponding frequency. By measuring the scattering parameter S_{21} both the dielectric constant (ε_r) and loss tangent (tanδ) of the substrate under test can be determined. This is possible because the former is related to the frequency point of the resonance, while the latter is related to the Q-factor of the resonator. A lab-made instrument [62] exploiting this method has been used to characterize the material, previously cast in the form of a substrate of size 100x50x3 mm^3. Dielectric constant and tanδ values have been used to define the new dielectric material in a full-wave simulation software, allowing the precise simulation of the final device which has been chosen to be a wideband monopolar antenna, whose design was previously published in [65].

4.2.23. Cell culture and biocompatibility assay

HepG2 cell line were maintained in high-glucose Dulbecco's Modified Eagle's Medium (HG-DMEM D5796, Sigma-Aldrich, Milano, Italy), supplemented with 10 % Fetal Bovine Serum (FBS), penicillin/streptomycin (100 IU/ml), and 2 mM L-glutamine, and incubated at 37 °C with 5 % CO_2. Cell proliferation assay was performed by using the 3-[4,5-

dimethylthiazol-2-yl]-2,5 diphenyl tetrazolium bromide (MTT) test at different time points (1 and 3 days). MTT is a colorimetric method used to assess the cellular viability through the metabolic activity of viable cells in converting the yellow tetrazolium salt into an insoluble purple formazan precipitate. By spectrophotometric analysis, it is possible to quantitatively assess the intensity of the staining, which is related to the amount and vitality of cells.

Non-contact: To evaluate the biocompatibility and the eventual release of potentially toxic compounds over time, circle-shaped OleoPlast with a diameter of 15 mm and 0.5 mm thickness were put in contact with 500 μl of cell culture medium described above and left at 37 °C with 5 % CO_2 for 1 and 3 days. For each experimental condition, HepG2 cells were cultured at a density of 6×10^4 cells/well in a 24-well plate in HG-DMEM medium. After 24 h, the culture medium from each well was replaced with 500 μl of the conditioned medium obtained from the incubation with OleoPlast sample, whereas control cells (CTR) were incubated with fresh medium. After 24 h, the proliferation assay was performed by adding 5 mg/ml MTT that had been 1:10 diluted and after 2 h formazan crystals formed in the cells were dissolved in 1 ml acidified isopropanol (37 % HCl in isopropanol). The absorbance was measured at 570 nm using a Multiskan FC ELISA reader (Thermo Fisher Scientific, Rodano-Italy). The viability is shown as a percentage of absorbance relative to untreated CTR cells, which will be green for the Live/Dead assay and blue for the DAPI assay.

In-contact: Further investigations were done to exclude the cell cytotoxicity of OleoPlast directly added to HepG2 cells, (ISO 10993-5:2009). For this purpose, HepG2 cells were seeded at a density of 6×10^4 cells/well in a 24-well plate in HG-DMEM medium. After 24 of incubation, the culture medium was replaced with 500 μl of fresh medium together with 15 mm diameter OleoPlast. 20 % DMSO/full medium mixture was adopted as a positive control and pure culture medium was added as a negative control. All samples were incubated at 37 °C with 5 % CO_2 for 24 h. At the end of the incubation period, an MTT assay was performed to quantify the cell viability following the same protocol as described above. Furthermore, Live/Dead assay (Fixable Aqua Dead Cell Stain, Thermo Fisher, Hong Kong) and DAPI assay were used to qualitatively appreciate the cellular viability. In particular, live cells interact with the reactive dye only on the surface, showing a weak fluorescence signal, while cells with compromised membranes interact throughout their volume, observing a brighter signal.

4.3. Statistical analysis

The data are presented as the Mean ± Standard Deviation (SD) for the indicated number of experiments. The statistical analysis was conducted by using One Way ANOVA, followed by Tuckey's test for multiple c omparisons with respect to the control (CTRL). In all comparisons, $p < 0.05$ was considered statistically significant, and the significance level was reported when present.

CRediT authorship contribution statement

Leonardo Lamanna: Writing – review & editing, Writing – original draft, Visualization, Validation, Supervision, Project administration, Methodology, Investigation, Funding acquisition, Formal analysis, Data curation, Conceptualization. **Gabriele Corigliano:** Investigation, Data curation. **Athira Narayanan:** Investigation, Data curation. **Stefania Villani:** Investigation, Data curation. **Marco Friuli:** Writing – review & editing, Investigation, Formal analysis, Data curation. **Francesco P. Chietera:** Investigation, Data curation. **Benedetta Di Chiara Stanca:** Investigation, Data curation. **Laura Giannotti:** Investigation, Data curation. **Luisa Siculella:** Supervision, Funding acquisition. **Riccardo Colella:** Investigation, Data curation. **Luca Catarinucci:** Supervision, Resources. **Athanassia Athanassiou:** Supervision, Resources. **Pietro Cataldi:** Writing – review & editing, Investigation, Formal analysis, Data curation. **Christian Demitri:** Supervision, Resources. **Mario Caironi:** Writing – review & editing, Supervision. **Alessandro Sannino:** Supervision, Resources, Funding acquisition.

Declaration of competing interest

The authors declare the following financial interests/personal relationships which may be considered as potential competing interests: Leonardo Lamanna has patent pending to ND. If there are other authors, they declare that they have no known competing financial interests or personal relationships that could have appeared to influence the work reported in this paper.

Data availability

Data will be made available on request.

Acknowledgment

M.C. acknowledges support from European Research Council (ERC) under the European Union's Horizon 2020 research and innovation programme "ELFO", Grant Agreement No. 864299. P.C. acknowledges funding from the Marie Skłodowska-Curie actions (project name: Bio-ConTact, grant agreement no. 101022279) under the European Union's Horizon 2020 research and innovation programme. S.V. acknowledges funding from the Italian Minister of Research with the Ministerial Decree n. 351/2022 –PNRR Mission 4, Component 1. A.N. acknowledges the financial support from the PON scholarship funded from the resources allocated by the MUR (Ministry of University and Research) with the Ministerial Decree for ESF resources REACT-EU and funds from the University of Salento. The authors acknowledge Lara Marini for her help in performing DSC and TGA measurements.

Appendix A. Supplementary data

Supplementary data to this article can be found online at https://doi.org/10.1016/j.cej.2024.154988.

References

[1] M.J. Kirwan, S. Plant, J.W. Strawbridge, Plastics in food packaging, Food. Beverage Packaging Technol. (2011) 157–212.
[2] T. Someya, Z. Bao, G.G. Malliaras, The rise of plastic bioelectronics, Nature 540 (7633) (2016) 379–385.
[3] Q. Xia, C. Chen, Y. Yao, J. Li, S. He, Y. Zhou, T. Li, X. Pan, Y. Yao, L. Hu, A strong, biodegradable and recyclable lignocellulosic bioplastic, Nat. Sustainability 4 (7) (2021) 627–635.
[4] L. Lamanna, Recent progress in polymeric flexible surface acoustic wave devices: materials, processing, and applications, Adv. Mater. Technol. 2300362 (2023).
[5] J. Brahney, M. Hallerud, E. Heim, M. Hahnenberger, S. Sukumaran, Plastic rain in protected areas of the United States, Science 368 (6496) (2020) 1257–1260.
[6] M.S. Bank, D.M. Mitrano, M.C. Rillig, C. Sze Ki Lin, Y.S. Ok, Embrace complexity to understand microplastic pollution, Nature Rev. Earth Environ. 3 (11) (2022) 736–737.
[7] R. Geyer, J.R. Jambeck, K.L. Law, Production, use, and fate of all plastics ever made, Sci. Adv. 3 (7) (2017) e1700782.
[8] U. Salahuddin, J. Sun, C. Zhu, M. Wu, B. Zhao, P.X. Gao, Plastic recycling: a review on life cycle, methods, misconceptions, and techno-economic analysis, Adv. Sustain. Sys. 7 (7) (2023) 2200471.
[9] M. MacLeod, H.P.H. Arp, M.B. Tekman, A. Jahnke, The global threat from plastic pollution, Science 373 (6550) (2021) 61–65.
[10] J.-G. Rosenboom, R. Langer, G. Traverso, Bioplastics for a circular economy, Nat. Rev. Mater. 7 (2) (2022) 117–137.
[11] J.D. Sachs, G. Schmidt-Traub, M. Mazzucato, D. Messner, N. Nakicenovic, J. Rockström, Six transformations to achieve the sustainable development goals, Nat. Sustainability 2 (9) (2019) 805–814.
[12] P. Skoczinski, M. Carus, G. Tweddle, P. Ruiz, D. de Guzman, J. Ravenstijn, H. Käb, N. Hark, L. Dammer, A. Raschka, Bio-based Building Blocks and Polymers: global Capacities, Production and Trends 2022–2027, Ind. Biotechnol. 19 (4) (2023) 185–194.
[13] I. Pillin, N. Montrelay, A. Bourmaud, Y. Grohens, Effect of thermo-mechanical cycles on the physico-chemical properties of poly (lactic acid), Polym. Degrad. Stab. 93 (2) (2008) 321–328.
[14] Y. Zhu, C. Romain, C.K. Williams, Sustainable polymers from renewable resources, Nature 540 (7633) (2016) 354–362.

[15] G. Zhou, H. Zhang, Z. Su, X. Zhang, H. Zhou, L. Yu, C. Chen, X. Wang, A. Biodegradable, Waterproof, and Thermally Processable Cellulosic Bioplastic Enabled by Dynamic Covalent Modification, Adv. Mater. 2301398 (2023).
[16] D. Klemm, B. Heublein, H.P. Fink, A. Bohn, Cellulose: fascinating biopolymer and sustainable raw material, Angew. Chem. Int. Ed. 44 (22) (2005) 3358–3393.
[17] H. Seddiqi, E. Oliaei, H. Honarkar, J. Jin, L.C. Geonzon, R.G. Bacabac, J. Klein-Nulend, Cellulose and its derivatives: towards biomedical applications, Cellul. 28 (4) (2021) 1893–1931.
[18] H. Zhou, H. Tong, J. Lu, Y. Cheng, F. Qian, Y. Tao, H. Wang, Preparation of bio-based cellulose acetate/chitosan composite film with oxygen and water resistant properties, Carbohydr. Polym. 270 (2021) 118381.
[19] L. Lamanna, G. Pace, I.K. Ilic, P. Cataldi, F. Viola, M. Friuli, V. Galli, C. Demitri, M. Caironi, Edible cellulose-based conductive composites for triboelectric nanogenerators and supercapacitors, Nano Energy 108168 (2023).
[20] A. Narayanan, M. Friuli, A. Sannino, C. Demitri, L. Lamanna, Green synthesis of stretchable Ethyl cellulose film plasticized with Transesterified Sunflower Oil, Carbohydrate Polymer Technologies and Applications 100378 (2023).
[21] A. Singh, F.-I. Auzanneau, M. Rogers, Advances in edible oleogel technologies–A decade in review, Food Res. Int. 97 (2017) 307–317.
[22] L. Lamanna, F. Rizzi, C. Demitri, M. Pisanello, E. Scarpa, A. Qualtieri, A. Sannino, M. De Vittorio, Determination of absorption and structural properties of cellulose-based hydrogel via ultrasonic pulse-echo time-of-flight approach, Cellul. 25 (8) (2018) 4331–4343, https://doi.org/10.1007/s10570-018-1874-4.
[23] A.J. Gravelle, A.G. Marangoni, M. Davidovich-Pinhas, Ethylcellulose oleogels, Elsevier, Edible oleogels, 2018, pp. 331–362.
[24] W. Zhao, Z. Wei, C. Xue, Y. Meng, Development of food-grade oleogel via the aerogel-templated method: oxidation stability, astaxanthin delivery and emulsifying application, Food Hydrocoll. 134 (2023) 108058.
[25] S. Manzoor, F. Masoodi, F. Naqash, R. Rashid, Oleogels: promising alternatives to solid fats for food applications, Food Hydrocolloids for Health 2 (2022) 100058.
[26] W. Zhao, Z. Wei, C. Xue, Recent advances on food-grade oleogels: fabrication, application and research trends, Crit. Rev. Food Sci. Nutr. 62 (27) (2022) 7659–7676.
[27] T.J. Silva, D. Barrera-Arellano, A.P.B. Ribeiro, Oleogel-based emulsions: concepts, structuring agents, and applications in food, J. Food Sci. 86 (7) (2021) 2785–2801.
[28] J. Santos, I. Santos, M. Conceição, S. Porto, M.F. Trindade, A. Souza, S. Prasad, V. Fernandes, A. Araújo, Thermoanalytical, kinetic and rheological parameters of commercial edible vegetable oils, J. Therm. Anal. Calorim. 75 (2004) 419–428.
[29] H. Yalcin, O.S. Toker, M. Dogan, Effect of oil type and fatty acid composition on dynamic and steady shear rheology of vegetable oils, J. Oleo Sci. 61 (4) (2012) 181–187.
[30] B. Ganesan, C. Brothersen, D.J. McMahon, Fortification of foods with omega-3 polyunsaturated fatty acids, Crit. Rev. Food Sci. Nutr. 54 (1) (2014) 98–114.
[31] M. Kervran, C. Vagner, M. Cochez, M. Ponçot, M.R. Saeb, H. Vahabi, Thermal degradation of polylactic acid (PLA)/polyhydroxybutyrate (PHB) blends: a systematic review, Polym. Degrad. Stab. 201 (2022) 109995.
[32] P.J. Flory, Principles of polymer chemistry, Cornell University Press, 1953.
[33] G.C. de Carvalho, M.d.F.V. de Moura, H.G.C. de Castro, J.H. da Silva Júnior, H.E. B. da Silva, K.M. dos Santos, Z.M.S. Rocha, Influence of the atmosphere on the decomposition of vegetable oils: study of the profiles of FTIR spectra and evolution of gaseous products, J. Therm. Anal. Calorim. 140 (5) (2020) 2247–2258.
[34] B. Ahmad, O. Gunduz, S. Stoyanov, E. Pelan, E. Stride, M. Edirisinghe, A novel hybrid system for the fabrication of a fibrous mesh with micro-inclusions, Carbohydr. Polym. 89 (1) (2012) 222–229.
[35] V. Dubois, S. Breton, M. Linder, J. Fanni, M. Parmentier, Fatty acid profiles of 80 vegetable oils with regard to their nutritional potential, Eur. J. Lipid Sci. Technol. 109 (7) (2007) 710–732.
[36] M.K. Mitchell, D.E. Hirt, Degradation of PLA fibers at elevated temperature and humidity, Polym. Eng. Sci. 55 (7) (2015) 1652–1660.
[37] H. Ventura, J. Claramunt, M. Rodríguez-Pérez, M. Ardanuy, Effects of hydrothermal aging on the water uptake and tensile properties of PHB/flax fabric biocomposites, Polym. Degrad. Stab. 142 (2017) 129–138.
[38] C.G. Amza, A. Zapciu, F. Baciu, M.I. Vasile, D. Popescu, Aging of 3D printed polymers under sterilizing UV-C radiation, Polymers 13 (24) (2021) 4467.
[39] M. Yu, Y. Zheng, J. Tian, Study on the biodegradability of modified starch/polylactic acid (PLA) composite materials, RSC Adv. 10 (44) (2020) 26298–26307.
[40] M. Gahleitner, J. Fiebig, J. Wolfschwenger, G. Dreiling, C. Paulik, Post-crystallization and physical aging of polypropylene: material and processing effects, J. Macromol. Sci. Part B 41 (4–6) (2002) 833–849.
[41] J. Rault, The αc transition in semicrystalline polymers: a new look at crystallization deformation and aging process, J. Macromol. Sci. Polym. Rev. 37 (2) (1997) 335–387.
[42] P. Saha, B.S. Kim, Preparation, characterization, and antioxidant activity of β-carotene impregnated polyurethane based on epoxidized soybean oil and malic acid, J. Polym. Environ. 27 (2019) 2001–2016.
[43] T.N. Nguyen, A. Rangel, D.W. Grainger, V. Migonney, Influence of spin finish on degradation, functionalization and long-term storage of polyethylene terephthalate fabrics dedicated to ligament prostheses, Sci. Rep. 11 (1) (2021) 4258.
[44] K.D. Sullivan, V. Gugliada, Fluorescence photobleaching of microplastics: a cautionary tale, Mar. Pollut. Bull. 133 (2018) 622–625.
[45] H. Luo, C. Liu, D. He, J. Sun, J. Li, X. Pan, Effects of aging on environmental behavior of plastic additives: migration, leaching, and ecotoxicity, Sci. Total Environ. 849 (2022) 157951.
[46] A.T.N. Do, Y. Ha, J.-H. Kwon, Leaching of microplastic-associated additives in aquatic environments: a critical review, Environ. Pollut. 305 (2022) 119258.
[47] F.M. Lamberti, L.A. Román-Ramírez, J. Wood, Recycling of bioplastics: routes and benefits, J. Polym. Environ. 28 (2020) 2551–2571.
[48] Z.O. Schyns, M.P. Shaver, Mechanical recycling of packaging plastics: a review, Macromol. Rapid Commun. 42 (3) (2021) 2000415.
[49] S. Budin, N. Maideen, M. Koay, D. Ibrahim, H. Yusoff, A comparison study on mechanical properties of virgin and recycled polylactic acid (PLA), Journal of Physics: Conference Series, IOP Publishing, 2019, p. 012002.
[50] F.P. La Mantia, M. Vinci, Recycling poly (ethyleneterephthalate), Polym. Degrad. Stab. 45 (1) (1994) 121–125.
[51] A. Honarbari, P. Cataldi, A. Zych, D. Merino, N. Paknezhad, L. Ceseracciu, G. Perotto, M. Crepaldi, A. Athanassiou, A green conformable thermoformed printed circuit board sourced from renewable materials, ACS Appl. Electron. Mater. (2023).
[52] G. Spallanzani, M. Najafi, M. Zahid, E.L. Papadopoulou, L. Ceseracciu, M. Catalano, A. Athanassiou, P. Cataldi, A. Zych, Self-Healing, Biodegradable, Electrically Conductive Vitrimer Coating for Soft Robotics, Advanced Sustainable Systems, Recyclable, 2023.
[53] L. Savenkova, Z. Gercberga, V. Nikolaeva, A. Dzene, I. Bibers, M. Kalnin, Mechanical properties and biodegradation characteristics of PHB-based films, Process Biochem. 35 (6) (2000) 573–579.
[54] L.K. Ncube, A.U. Ude, E.N. Ogunmuyiwa, R. Zulkifli, I.N. Beas, Environmental impact of food packaging materials: a review of contemporary development from conventional plastics to polylactic acid based materials, Materials 13 (21) (2020) 4994.
[55] E.P.o.F. Additives, N.S.a.t. Food, M. Younes, P. Aggett, F. Aguilar, R. Crebelli, A. Di Domenico, B. Dusemund, M. Filipič, M. Jose Frutos, P. Galtier, Re-evaluation of celluloses E 460 (i), E 460 (ii), E 461, E 462, E 463, E 464, E 465, E 466, E 468 and E 469 as food additives, EFSA Journal 16(1) (2018) e05047.
[56] V. Goudarzi, I. Shahabi-Ghahfarrokhi, A. Babaei-Ghazvini, Preparation of ecofriendly UV-protective food packaging material by starch/TiO2 bio-nanocomposite: characterization, Int. J. Biol. Macromol. 95 (2017) 306–313.
[57] A.S. Sharova, F. Modena, A. Luzio, F. Melloni, P. Cataldi, F.A. Viola, L. Lamanna, N. F. Zorn, M. Sassi, C. Ronchi, Chitosan gated organic transistors printed on ethyl cellulose as a versatile platform for edible electronics and bioelectronics, Nanoscale (2023).
[58] I.K. Ilic, L. Lamanna, D. Cortecchia, P. Cataldi, A. Luzio, M. Caironi, Self-Powered Edible Defrosting Sensor, ACS sensors (2022).
[59] P. Cataldi, L. Lamanna, C. Bertei, F. Arena, P. Rossi, M. Liu, F. Di Fonzo, D.G. Papageorgiou, A. Luzio, M. Caironi, An Electrically Conductive Oleogel Paste for Edible Electronics, Advanced Functional Materials n/a(n/a) 2113417. https://doi.org/https://doi.org/10.1002/adfm.202113417.
[60] I.K. Ilic, V. Galli, L. Lamanna, P. Cataldi, L. Pasquale, V.F. Annese, A. Athanassiou, M. Caironi, An edible rechargeable battery, Adv. Mater. 2211400 (2023).
[61] L. Lamanna, P. Cataldi, M. Friuli, C. Demitri, M. Caironi, Monitoring of drug release via intra body communication with an edible Pill, Adv. Mater. Technol. 2200731 (2022).
[62] L. Catarinucci, R. Colella, P. Coppola, L. Tarricone, Microwave characterisation of polylactic acid for 3D-printed dielectrically controlled substrates, IET Microwaves Antennas Propag. 11 (14) (2017) 1970–1976.
[63] D. Qi, K. Zhang, G. Tian, B. Jiang, Y. Huang, Stretchable electronics based on PDMS substrates, Adv. Mater. 33 (6) (2021) 2003155.
[64] Y. Liu, X.-Y. Zhao, Y.-G. Sun, W.-Z. Li, X.-S. Zhang, J. Luan, Synthesis and applications of low dielectric polyimide, Resour. Chem. Mater. 2 (1) (2023) 49–62.
[65] B. Chen, Y.-C. Jiao, F.-C. Ren, L. Zhang, Broadband monopole antenna with wideband circular polarization, Progress In Electromagnetics, Res. Lett. 32 (2012) 19–28.
[66] F. Hirtenfelder, Effective antenna simulations using CST MICROWAVE STUDIO®, 2007 2nd International ITG Conference on Antennas, IEEE, 2007, pp. 239-239.
[67] P. Cataldi, J.A. Heredia-Guerrero, S. Guzman-Puyol, L. Ceseracciu, L. La Notte, A. Reale, J. Ren, Y. Zhang, L. Liu, M. Miscuglio, Sustainable electronics based on crop plant extracts and graphene: a “bioadvantaged” approach, Advanced Sustainable Systems 2 (11) (2018) 1800069.
[68] J.T. Nandhini, D. Ezhilarasan, S. Rajeshkumar, An ecofriendly synthesized gold nanoparticles induces cytotoxicity via apoptosis in HepG2 cells, Environ. Toxicol. 36 (1) (2021) 24–32.
[69] T. Wang, M. Ma, C. Chen, X. Yang, Y. Qian, Three widely used pesticides and their mixtures induced cytotoxicity and apoptosis through the ROS-related caspase pathway in HepG2 cells, Food Chem. Toxicol. 152 (2021) 112162.
[70] R. Podgórski, M. Wojasiński, T. Ciach, Nanofibrous materials affect the reaction of cytotoxicity assays, Sci. Rep. 12 (1) (2022) 9047.
[71] R. Guarnieri, R. Reda, D. Di Nardo, G. Miccoli, A. Zanza, L. Testarelli, In vitro direct and indirect cytotoxicity comparative analysis of one pre-hydrated versus one dried acellular porcine dermal matrix, Materials 15 (5) (2022) 1937.
[72] Z. Ma, Q. Huang, Q. Xu, Q. Zhuang, X. Zhao, Y. Yang, H. Qiu, Z. Yang, C. Wang, Y. Chai, Permeable superelastic liquid-metal fibre mat enables biocompatible and monolithic stretchable electronics, Nat. Mater. 20 (6) (2021) 859–868.
[73] V. Shanmugam, R.A. Mensah, M. Försth, G. Sas, Á. Restás, C. Addy, Q. Xu, L. Jiang, R.E. Neisiany, S. Singha, Circular economy in biocomposite development: state-of-the-art, challenges and emerging trends, Composites Part c: Open Access 5 (2021) 100138.
[74] M.J. John, S. Thomas, Biofibres and biocomposites, Carbohydr. Polym. 71 (3) (2008) 343–364.
[75] J. Payá, J. Roselló, J.M. Monzó, A. Escalera, M.P. Santamarina, M.V. Borrachero, L. Soriano, An approach to a new supplementary cementing material: arundo donax straw ash, Sustainability 10 (11) (2018) 4273.

[76] M. Chiumarelli, M.D. Hubinger, Evaluation of edible films and coatings formulated with cassava starch, glycerol, carnauba wax and stearic acid, Food Hydrocoll. 38 (2014) 20–27.
[77] S. Despond, E. Espuche, N. Cartier, A. Domard, Barrier properties of paper–chitosan and paper–chitosan–carnauba wax films, J. Appl. Polym. Sci. 98 (2) (2005) 704–710.
[78] K. Faraj, M. Khaled, J. Faraj, F. Hachem, C. Castelain, Phase change material thermal energy storage systems for cooling applications in buildings: a review, Renew. Sustain. Energy Rev. 119 (2020) 109579.
[79] G. Tedeschi, S. Guzman-Puyol, L. Ceseracciu, J.J.s. Benitez, P. Cataldi, M. Bissett, A. Heredia, A. Athanassiou, J.A. Heredia-Guerrero, Sustainable, high-barrier polyaleuritate/nanocellulose biocomposites, ACS Sustain. Chem. Eng. 8 (29) (2020) 10682–10690.
[80] R. Colella, F.P. Chietera, L. Catarinucci, Analysis of FDM and DLP 3D-printing technologies to prototype electromagnetic devices for RFID applications, Sensors 21 (3) (2021) 897.